Constraining feeble neutrino interactions with ultralight dark matter

Abhish Dev[1,*] Gordan Krnjaic,[1,2,3,†] Pedro Machado[1,‡] and Harikrishnan Ramani[4,§]

[1]*Theoretical Physics Department, Fermi National Accelerator Laboratory, Batavia, Illinois 60510, USA*
[2]*Department of Astronomy and Astrophysics, University of Chicago, Chicago, Illinois 60637, USA*
[3]*Kavli Institute for Cosmological Physics, University of Chicago, Chicago, Illinois 60637, USA*
[4]*Stanford Institute for Theoretical Physics, Stanford University, Stanford, California 94305, USA*

If ultralight ($\ll$ eV), bosonic dark matter couples to right-handed neutrinos, active neutrino masses and mixing angles depend on the ambient dark matter density. When the neutrino Majorana mass, induced by the dark matter background, is small compared to the Dirac mass, neutrinos are "pseudo-Dirac" fermions that undergo oscillations between nearly degenerate active and sterile states. We present a complete cosmological history for such a scenario and find severe limits from a variety of terrestrial and cosmological observables. For scalar masses in the "fuzzy" dark matter regime ($\sim 10^{-20}$ eV), these limits exclude couplings of order 10^{-30}, corresponding to Yukawa interactions comparable to the gravitational force between neutrinos and surpassing equivalent limits on time variation in scalar-induced electron and proton couplings.

I. INTRODUCTION

The identity of dark matter and the origin of neutrino masses are two fundamental mysteries that unambiguously require new physics beyond the Standard Model (SM). Unlike other deficiencies of the SM (e.g., the lack of an inflaton candidate), these problems may be resolved with interactions at terrestrially and astrophysically accessible energy scales. Thus, exploring all viable connections between these problems is generically interesting, especially when they economically combine known tools that address each problem separately.

Ultralight ($\ll$ eV) bosonic dark matter (DM) ϕ is characterized by a macroscopic de Broglie wavelength

$$\lambda_\phi = \frac{1}{m_\phi v_\phi} \approx 200 \text{ km} \left(\frac{\text{neV}}{m_\phi} \right) \left(\frac{10^{-3}}{v_\phi} \right), \quad (1)$$

which exceeds the interparticle separation, where v_ϕ is the field velocity. If ϕ is misaligned from the minimum of quadratic potential, it oscillates as a classical field about this minimum according to

$$\phi(\vec{r}, t) = \frac{\sqrt{2\rho_\phi(t)}}{m_\phi} \cos[m_\phi(t + \vec{v}_\phi \cdot \vec{r}) + \varphi(\vec{r})], \quad (2)$$

and the corresponding energy density redshifts like non-relativistic matter $\rho_\phi \propto a^{-3}$, where a is the cosmic scale factor and φ is a possible phase. This phase may encode additional information about spatial variation—e.g., different ϕ domains arising from cosmological initial conditions[1] or the incoherent virialization in the Galaxy leading to variation on the scale of λ_ϕ.

If ϕ couples to SM particles, their masses, spins, and coupling constants may inherit time dependence from Eq. (2). In the context of charged SM particles, there are many searches for such phenomena, which typically place very strong limits on the ϕ-SM interaction strength (see Ref. [1] for a review). By contrast, there are relatively few bounds on DM-induced time dependence in the neutrino sector [2–15] and the corresponding limits constrain comparatively large interaction strengths primarily via flavor oscillations.

In this paper, we introduce the possibility that an ultralight DM candidate ϕ induces a time-dependent Majorana mass for right-handed neutrinos,

$$m_M = \frac{y_\phi}{2} \phi(t), \quad (3)$$

*abhish@fnal.gov
†krnjaicg@fnal.gov
‡pmachado@fnal.gov
§hramani@stanford.edu

---

[1]This can happen, e.g., due to oscillation starting at slightly different times in different Hubble patches when the field becomes dynamical at $H \sim m_\phi$.

where y_ϕ is a coupling constant and the time dependence arises from Eq. (2). Since misaligned scalar fields must be thermally decoupled from SM particles, they can only induce a tiny Majorana mass without spoiling their cold cosmic abundance through interactions with neutrinos. This requirement eliminates many possible connections between neutrinos and ultralight dark matter, but is compatible with the pseudo-Dirac regime, which is the focus of our paper.

When the neutrino Majorana mass is small compared to the Dirac mass m_D, the mass eigenstates form a pair of pseudo-Dirac fermions; one "active" ν_a and one "sterile" ν_s (per generation). These states oscillate into each other with a characteristic probability governed by their squared mass difference δm^2 [16],

$$P(\nu_a \to \nu_s) = \sin^2(2\theta) \sin^2\left(\frac{\delta m^2 L}{4E_\nu}\right), \qquad (4)$$

where L is the baseline, E_ν is the energy of the propagating neutrino, and $\theta \approx \pi/4$ is the mixing angle, which is near maximal in the pseudo-Dirac limit where $m_M \ll m_D$.

The Majorana mass governing δm^2 in Eq. (4) is time dependent, so the oscillation rate becomes sensitive to the dark matter density and to its cosmic evolution. This dependence can impact various terrestrial and cosmological observables. In this work, we extract resultant bounds and impose *extremely* strong limits on the induced Majorana mass; depending on the value of m_ϕ, we find some limits on the coupling y_ϕ corresponding to a ϕ mediated Yukawa force comparable to that of gravity.

This paper is organized as follows: in Sec. II we present our theoretical framework, in Sec. III we delineate the qualitatively different neutrino oscillation regimes that ϕ can induce, in Sec. IV we compute the terrestrial bounds, in Sec. V we determine the cosmological bounds on this scenario, and in Sec. VI we make some concluding remarks.

II. ULTRALIGHT DARK MATTER AND PSEUDO-DIRAC NEUTRINOS

We consider a scalar DM candidate ϕ with lepton number 2 and a cosmic abundance due to misalignment. In Weyl fermion notation, the Lagrangian in this scenario contains

$$\mathcal{L} \supset y_\nu H \ell N + \frac{y_\phi}{2} \phi NN + \text{H.c.}, \qquad (5)$$

where y_ν is the neutrino Yukawa coupling, H is the SM Higgs doublet, ℓ is the SM lepton doublet, and N is a SM neutral fermion, i.e., a right-handed neutrino. As we will see next, the presence of a feeble interaction between the scalar DM and the right-handed neutrino can have dramatic effects in neutrino oscillation phenomenology.

To understand the impact of ϕ on neutrino oscillations, it is instructive to describe the "1 + 1" scenario, in which there is only one generation of ℓ and N. For simplicity, assume that the active state here is an electron flavor neutrino. In the broken electroweak phase, the first term in Eq. (5) generates a Dirac mass of neutrinos. When the ϕ field is misaligned according to Eq. (2), the second term in Eq. (5) generates a Majorana mass for N, so we have

$$m_D = \frac{y_\nu v}{\sqrt{2}}, \qquad m_M = \frac{y_\phi}{2} \phi(t), \qquad (6)$$

for the Dirac and Majorana contributions, respectively, where $v = 246$ GeV is the Higgs vacuum expectation value. When $m_M \ll m_D$, we obtain two nearly degenerate neutrino mass-squared eigenstates

$$m^2_{h,\ell} = m^2_D \pm m_D m_M \equiv m^2_\nu \pm \frac{1}{2}\delta m^2, \qquad (7)$$

and we define $\delta m^2 \equiv y_\phi m_D \sqrt{2\rho_\phi}/m_\phi$, where

$$\delta m^2 \approx 2 \times 10^{-15} \text{ eV}^2 \left(\frac{y_\phi}{10^{-10}}\right) \left(\frac{10^{-15} \text{ eV}}{m_\phi}\right) \left(\frac{m_D}{0.1 \text{ eV}}\right), \quad (8)$$

for the splitting between Weyl fermions, as opposed to the usual Δm^2_{ij} measured in oscillation experiments; here we have taken the local density to be $\rho^\odot_\phi = 0.4$ GeV/cm^3 [17]. The active-sterile mixing angle in this case is

$$\tan(2\theta) = \frac{2m_D}{m_M} \gg 1, \qquad (9)$$

which is nearly maximal, $\theta \approx \pi/4$ in our full parameter space of interest.

The diagonalization of the mass terms in Eq. (6) is obtained by defining the flavor fields in terms of the mass eigenstates approximately as

$$|\nu_e\rangle = \frac{1}{\sqrt{2}}(|\nu_h\rangle + |\nu_\ell\rangle), \qquad (10)$$

$$|\nu_s\rangle = \frac{1}{\sqrt{2}}(|\nu_h\rangle - |\nu_\ell\rangle). \qquad (11)$$

The time evolution of a ν_e state is given by

$$U(t)|\nu_e\rangle = \frac{1}{\sqrt{2}}\left[\exp\left(-\frac{i}{2E_\nu}\int_0^t dt' m_1^2(t')\right)|\nu_1\rangle \right.$$
$$\left. + \exp\left(-\frac{i}{2E_\nu}\int_0^t dt' m_2^2(t')\right)|\nu_2\rangle\right], \qquad (12)$$

which yields a $\nu_e \to \nu_e$ survival probability

$$P_{ee}(t) = |\langle \nu(t)|\nu_e\rangle|^2 = \cos^2\left(\frac{1}{4E_\nu}\int_0^t dt' \delta m^2(t')\right). \quad (13)$$

Using Eqs. (2) and (6) we obtain

$$\frac{1}{2}\int_0^t dt' \delta m^2(t') = \frac{y_\phi m_D}{m_\phi}\sqrt{2\rho_\phi}\int_0^t dt' \cos(m_\phi t' + \varphi),$$

where we have absorbed the v_ϕ dependence in Eq. (2) into the definition of φ for brevity. Thus, for a neutrino emitted at $t = 0$ and observed at some later time t, the resulting electron-neutrino disappearance probability can be written as

$$1 - P_{ee} = \sin^2\left\{\frac{m_D}{2E_\nu}\frac{y_\phi\sqrt{2\rho_\phi}}{m_\phi^2}(\sin[m_\phi t + \varphi] - \sin\varphi)\right\}, \quad (14)$$

where we have treated the phase φ as a constant over the propagation time.

Generalization for more neutrino flavors is straightforward and can be derived following similar steps as those taken in Ref. [18]. Moreover, to simplify the discussion on the constraints and because the electron-neutrino admixture in ν_3 is small ($|U_{e3}| \ll 1$), when ϕ couples to ν_1 or ν_2 we will only consider nonstandard ν_e disappearance, while when ϕ couples to ν_3 we will only consider nonstandard $\nu_{\mu,\tau}$ disappearance; in both regimes, we treat the active-sterile oscillation in a two-flavor (active-sterile) framework.

As written in Eq. (2), the phase φ need not be constant over the full neutrino trajectory. Indeed, in the Galaxy, virialization will disrupt any constant phase value down to coherence patches of order the de Broglie wavelength in Eq. (1). Thus, the full oscillation probability will depend crucially on the relative size of the oscillation baseline and this coherence scale.

Finally, we note that our scalar mass is not protected by any symmetry, so it will be sensitive to irreducible one-loop corrections of order

$$\delta m_\phi \sim \frac{y_\phi m_D}{4\pi} \sim 10^{-18} \text{ eV}\left(\frac{y_\phi}{10^{-15}}\right)\left(\frac{m_D}{10 \text{ meV}}\right), \quad (15)$$

from the interactions in Eq. (5). Thus, for small y_ϕ in the pseudo-Dirac limit, this contribution does not destabilize the ultralight scalar mass, assuming no ϕ couplings to heavier states.[2]

---

[2]The operator $kH^\dagger H|\phi|^2$ is also allowed by all symmetries and can induce a large correction to m_ϕ if the coefficient is not suppressed. Exponential $k \ll 1$ suppression can be achieved in UV models where H and ϕ are localized on different branes in a higher-dimensional spacetime.

III. NEUTRINO OSCILLATION REGIMES

In what follows, we will consider three distinct regimes for neutrino oscillations in the presence of the ultralight scalar fields. These regimes arrive from the relation between the neutrino oscillation length and the modulation frequency of ϕ or the coherence length that defines the overall phase φ. Instead of performing a detailed fit of experimental data, we will recast existing constraints on pseudo-Dirac neutrinos from Ref. [19] on our parameters of interest, y_ϕ and m_ϕ. As neutrinos are ultrarelativistic, we identify $t = L$ in Eq. (14).

A. Constant ϕ: $m_\phi L \lesssim 1$

In the low-frequency $m_\phi L \lesssim 1$ regime, the neutrino encounters a constant phase φ domain over the course of its propagation. Expanding Eq. (14) around $m_\phi L \to 0$ yields an oscillation probability

$$1 - P_{ee} \approx \sin^2\left(\frac{L}{4E_\nu}\frac{2y_\phi m_D}{m_\phi}\sqrt{2\rho_\phi}\cos\varphi\right). \quad (16)$$

We can interpret this oscillation probability as follows. Since the period of the field ϕ is too long compared to the neutrino time of flight, the pseudo-Dirac mass splitting induced by the field is constant for each neutrino. Nevertheless, as an experiment collects data, the mass splitting will evolve as the field ϕ displays time modulation. In practice, several neutrino experiments have a high enough rate of events to observe time modulation of oscillation probabilities with periods as short as 10 min, which would correspond to $m_\phi \sim 10^{-18}$ eV [3–5,12]. Since any small pseudo-Dirac mass splitting leads to maximal mixing, time modulation of neutrino oscillation probabilities due to ϕ modulation would lead to large, observable effects on oscillation data.

Both constant and time-dependent pseudo-Dirac mass splittings would be ruled out by neutrino data if observed and can be used to set limits on the coupling strength y_ϕ for a given m_ϕ. Since sterile neutrino oscillation constraints are typically reported as bounds on δm^2, we can define an effective mass-squared δm_{eff}^2 by equating the arguments of Eqs. (4) and (16) to obtain

$$\delta m_{\text{eff}}^2 \equiv \frac{2y_\phi m_D}{m_\phi}\sqrt{2\rho_\phi}, \quad (17)$$

assuming $\cos\varphi \sim 1$. Recasting pseudo-Dirac neutrino limits on δm^2 in Eq. (17) allows us to constrain

$$y_\phi < \frac{m_\phi}{2m_D}\frac{\delta m_{\text{lim}}^2}{\sqrt{2\rho_\phi}}, \quad (18)$$

where we have identified δm_{eff}^2 with the constrained value δm_{lim}^2. Note that, depending on context, ρ_ϕ can either be the

cosmological DM density at a given cosmic era or the present day local density.

B. Modulating ϕ: $(m_\phi v_\phi L < 1 \ll m_\phi L)$

When the ϕ modulating frequency is high, $m_\phi L \gg 1$, the accumulated phase due to propagation is sufficient to induce many modulation cycles on ϕ over the neutrino trajectory. However, as long as $m_\phi v_\phi L \lesssim 1$, the neutrino time of flight is shorter than separation time of ϕ wave packets. A neutrino propagating in this regime will encounter the same value of φ across its trajectory; that is, the modulation of ϕ throughout the neutrino trajectory is coherent. Without loss of generality, we can set the initial condition $\varphi = 0$. The effective oscillation probability in this regime is given by a time average of Eq. (14) over the duration of propagation,

$$\langle 1 - P_{ee} \rangle \approx \sin^2 \left(\frac{y_\phi m_D}{2 E_\nu m_\phi^2} \sqrt{2\rho_\phi} \right), \qquad (19)$$

where we have assumed that ρ_ϕ does not change appreciably across the baseline. In this intermediate regime, we repeat the argument leading up to Eq. (18) and constrain

$$y_\phi^{\text{lim}} = \frac{\delta m_{\text{lim}}^2 m_\phi^2 L}{2 m_D \sqrt{2\rho_\phi}}. \qquad (20)$$

C. Random walk: $1 \ll m_\phi v_\phi L$

Finally, in the $m_\phi v_\phi L \gg 1$ regime, the neutrino time of flight is longer than the wave packet separation of ϕ, so the neutrino traverses a random sample of ϕ field patches, each with a different phase φ. Along this trajectory, there are approximately $m_\phi v_\phi L$ patches whose contributions add incoherently, so the effective phase can be approximated by $\varphi_{\text{eff}} \sim \sqrt{m_\phi v_\phi L}$, assuming random distribution of phases φ and the phase-averaged probability can be written

$$\langle 1 - P_{ee} \rangle \approx \sin^2 \left(\frac{y_\phi m_D \sqrt{2\rho_\phi v_\phi L}}{2 E_\nu m_\phi^{3/2}} \right). \qquad (21)$$

The corresponding limit on the coupling reads

$$y_\phi^{\text{lim}} = \frac{\delta m_{\text{lim}}^2}{m_D} \sqrt{\frac{m_\phi^3 L}{2\rho_\phi v_\phi}}. \qquad (22)$$

IV. TERRESTRIAL OBSERVABLES

We now consider various terrestrial bounds on pseudo-Dirac neutrinos in the context of our scenario. Depending on the values of y_ϕ and m_ϕ, a particular constraint can apply

in any of the three regimes outlined in Sec. III, so the relationship between y_ϕ and m_ϕ will differ in each case.

A. Solar neutrinos

For electron neutrinos, the pseudo-Dirac splitting can be constrained by measurements of the solar neutrino flux. In the standard three neutrino oscillations paradigm, ^{8}B neutrinos undergo an adiabatic evolution due to large matter effects in the Sun [20]. This leads to a survival probability $P(\nu_e \to \nu_e) \simeq c_{13}^4 s_{12}^2 + s_{13}^4 \simeq 0.3$, where s_{ij} and c_{ij} are the sines and cosines of mixing angle θ_{ij}. Low-energy solar neutrinos, on the other hand, are not affected by matter effects, and thus $P(\nu_e \to \nu_e) \simeq c_{13}^4 (c_{12}^4 + s_{12}^4) + s_{13}^4 \simeq 0.55$. These probabilities describe well the experimental data [21–29]. This can be used to extract an order of magnitude bound on the splitting in our scenario by demanding that this prediction is not affected by an order 1 amount. Here we use $\rho_\phi^\odot$ and $v_\phi \approx 10^{-3}$ with $L = 1.5 \times 10^8$ km, which requires

$$\delta m_{\text{lim}}^2 < 10^{-12} \text{ eV}^2 \qquad (23)$$

and can be translated into a bound on our model parameters using the relations in Sec. III, where the appropriate regime is determined by m_ϕ. Since solar neutrinos are essentially almost pure ν_2 or incoherent ν_e, and ν_e has but a small admixture ν_3 mass eigenstate, the corresponding solar limit on the y_ϕ applies only to the right-handed partners $N_{1,2}$. Applying the solar limit from Eq. (23) to the three regimes from Sec. III A, and assuming that the Dirac mass of ν_1 satisfies $m_D^2 = \Delta m_{21}^2 = 7.4 \times 10^{-5}$ eV^2 [30], we find the following constraints.

For $m_\phi \lesssim 10^{-18}$ eV, solar neutrinos are in the constant ϕ regime, so from Eq. (18), we find a limit

$$y_\phi^{\text{lim}} \approx 3 \times 10^{-26} \left(\frac{m_\phi}{10^{-18} \text{ eV}} \right), \quad \text{for } m_\phi < 10^{-18} \text{ eV.} \quad (24)$$

Note that, if $m_\phi \lesssim 10^{-24}$ eV, the period of ϕ is larger than 20 yr, and the observation of pseudo-Dirac mass splittings become dependent on the initial condition φ. For $10^{-18} \lesssim m_\phi \lesssim 10^{-15}$ eV, we are in the modulating ϕ regime, where Eq. (20) yields a limit of order

$$y_\phi^{\text{lim}} \approx 3 \times 10^{-26} \left(\frac{m_\phi}{10^{-18} \text{ eV}} \right)^{1/2}, \quad \text{for } m_\phi < 10^{-15} \text{ eV.} \quad (25)$$

Finally, for $m_\phi \gtrsim 10^{-15}$ eV, solar neutrinos will traverse a random sample of phases φ, corresponding to the random walk regime, so the bound from Eq. (22) applies to give

$$y_\phi^{\text{lim}} \approx 2 \times 10^{-20} \left(\frac{m_\phi}{10^{-15} \text{ eV}} \right)^{3/2}, \quad \text{for } m_\phi > 10^{-15} \text{ eV.} \quad (26)$$

These results are plotted in the left panel of Fig. 1, which shows constraints on ϕ coupled only to ν_1 or ν_2, corresponding to ν_e oscillations measurements.

B. Atmospheric neutrinos

Measurements of the atmospheric neutrinos can place limits on the ϕ coupling to ν_3 since muon neutrinos have a large admixture of the ν_3 eigenstate. If ν_3 is split in a pseudo-Dirac pair, a substantial deficit of atmospheric ν_μ flux would be observed, contradicting experimental data [33–36]. The characteristic atmospheric baseline is Earth's radius $L \approx 6000$ km, and the Super-Kamiokande constraint on constant pseudo-Dirac mass splittings is [19]

$$\delta m^2_{\text{lim}} < 10^{-4} \text{ eV}^2, \tag{27}$$

which translates into a bound on the ϕ coupling to ν_3. For ultralight ϕ masses, atmospheric oscillations are in the constant ϕ regime of Sec. III A, so translating the constraint from Eq. (27) with Dirac mass satisfying $m^2_D = \Delta m^2_{32} = 2.4 \times 10^{-3} \text{ eV}^2$ [30] yields

$$y^{\text{lim}}_\phi \approx 10^{-14} \left(\frac{m_\phi}{3 \times 10^{-14} \text{ eV}} \right), \tag{28}$$

which is valid for $m_\phi \lesssim 3 \times 10^{-14}$ eV. For larger ϕ masses in the modulating ϕ regime of Sec. III B, we impose the limit

$$y^{\text{lim}}_3 \approx 10^{-14} \left(\frac{m_\phi}{3 \times 10^{-14} \text{ eV}} \right)^2. \tag{29}$$

These bounds are presented in the orange shaded region of Fig. 1 (right panel). Note that for $m_\phi \gtrsim 10^{-10}$ eV, atmospheric oscillations are in the long baseline regime of Sec. III C, but the bound in this mass range is subdominant to other constraints in Fig. 1 and is not shown. In principle, atmospheric neutrinos also bound the ϕ coupling to $\nu_{1,2}$, but solar constraints are stronger.

V. COSMOLOGY

A. Scalar evolution

Throughout our analysis, we assume that the ϕ potential can be written as

$$V(\phi) = m^2_\phi |\phi|^2 + \frac{\lambda_\phi}{4} |\phi|^4 + \mathcal{O}(|\phi|^6), \tag{30}$$

where, in principle, the size of the quartic is unconstrained by symmetry arguments and can take on any value. However, there is an irreducible contribution to the quartic interaction generated through a Coleman-Weinberg interaction with the neutrinos

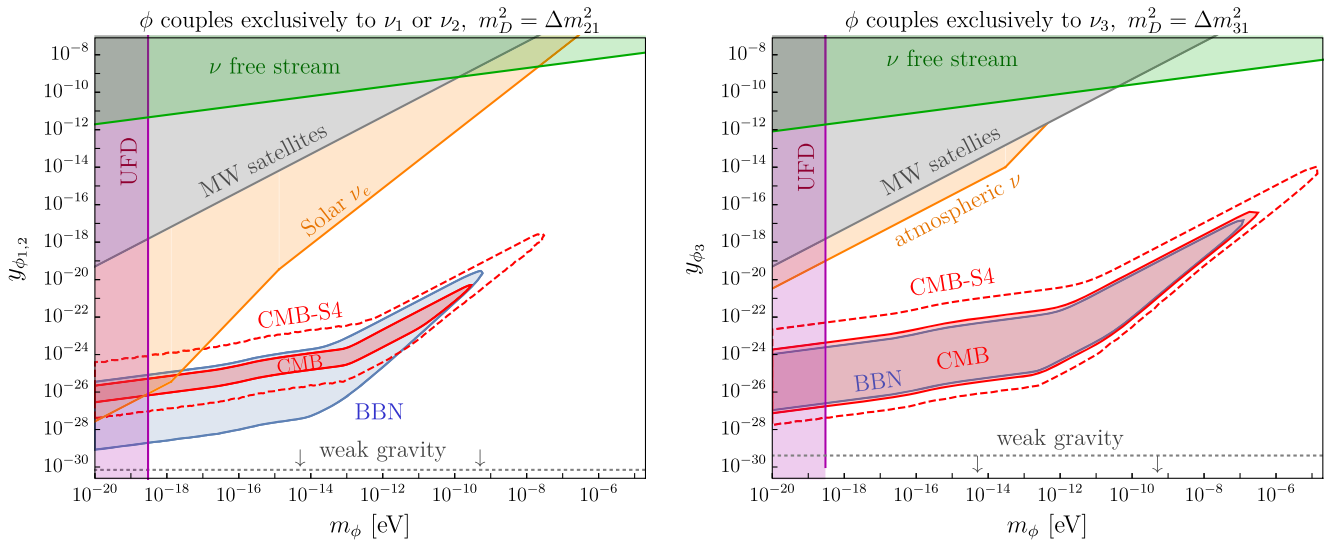$$\lambda^{\text{min}}_\phi \approx \frac{y^4_\phi}{16\pi^2}, \tag{31}$$

FIG. 1. Left: parameter space for ϕ coupled only to ν_1 or ν_2 mass eigenstates, which is predominantly constrained ν_e oscillation bounds. Here we show bounds from cosmic microwave background (CMB) and big bang nucleosynthesis (BBN) from Sec. V, Milky Way (MW) satellites from Sec. V B, scalar thermalization with neutrinos from Sec. V D, solar neutrino oscillations from Sec. IV A, and model-independent limits on light DM from ultrafaint dwarf (UFD) heating [31]. For points below the gray dotted line, the ϕ mediated force between right-handed neutrinos is weaker than gravity, which is theoretically disfavored by the weak gravity conjecture [32] Right: same as the left, only ϕ now couples only to ν_3, so the limits are driven by $\nu_{\mu,\tau}$ oscillations for which the solar bound is subdominant to the atmospheric bound described in Sec. IV B.

which is always present in the absence of fine-tuning. In an expanding Friedmann-Robertson-Walker universe, ϕ satisfies the equation of motion

$$\ddot{\phi} + 3H\dot{\phi} + V' = 0, \tag{32}$$

where the prime denotes a derivative with respect to ϕ.

If ϕ is initially displaced from its minimum, it is frozen by Hubble friction until $H\dot{\phi} \sim V'$, so if the mass term dominates the potential, $V' \sim m_\phi^2 \phi$, the field becomes dynamical when $m_\phi \sim H$ and oscillates about $\phi = 0$ while redshifting like nonrelativistic matter $\rho_\phi \propto a^{-3}$.

In this scenario, the initial misalignment amplitude ϕ_i during inflation sets the DM abundance. Since $m_\phi/H_i \ll 1$, where H_i is the Hubble scale during inflation, ϕ generates isocurvature perturbations, which are constrained by CMB measurements [37]. However, as long as $\phi_i/H_i \gg 1$, isocurvature perturbations can be parametrically suppressed; so for a given H_i, a suitable choice of ϕ_i can account for the DM abundance while being safe from this constraint. Furthermore, since $m_\phi/H_i \ll 1$, ϕ evolution is predominantly classical during inflation, so the initial amplitude ϕ_i remains a free parameter throughout our analysis and can be chosen to yield the observed DM density [38].

B. Milky Way satellites

In order for ϕ to account for the full DM abundance, it must redshift like nonrelativistic matter ($\rho_\phi \propto a^{-3}$) in the early Universe, starting at least at matter-radiation equality at a critical redshift $z_\star \sim 10^6$, corresponding to a temperature $T_\star \sim$ keV [39]. Since the ϕNN interaction in Eq. (5) yields an irreducible quartic scalar self-interaction term, we need to ensure that the ρ_ϕ is not dominated by the quartic contribution at T_{eq}; otherwise, it would redshift like radiation $\rho_\phi \propto a^{-4}$ (or faster if even higher polynomial terms dominate instead) [40]. Avoiding this fate requires

$$m_\phi^2 |\phi_\star|^2 > \frac{y_\phi^4}{16\pi^2} |\phi_\star|^4, \tag{33}$$

where $\phi_\star \equiv \phi(T_\star)$. Using the scaling in Eq. (2), we find

$$y_\phi \lesssim \left[\frac{8\pi^2 m_\phi^4}{\Omega_{dm}\rho_c}\left(\frac{T_0}{T_\star}\right)^{3/2}\right]^{1/4} \approx 5 \times 10^{-9}\left(\frac{m_\phi}{\text{neV}}\right),$$
$$\lambda_\phi \lesssim 4 \times 10^{-36}\left(\frac{m_\phi}{\text{neV}}\right)^4, \tag{34}$$

where ρ_c is the present day critical density. The inequality in Eq. (34) defines the gray shaded regions in Fig. 1 where this effect would erase the Milky Way satellites already observed. However, note that this bound is model-dependent, as it can be evaded if ϕ is only a small fraction of the total dark matter abundance, in which case it need not redshift like nonrelativistic matter at early (or even later) times.

C. Black hole superradiance

The phenomenon of black hole superradiance, the growth of ultralight boson clouds around spinning black holes, has been used to set limits in certain regions of ultralight boson parameter space irrespective of the boson couplings to the Standard Model [41]. However, these limits apply only when the self-interactions are negligible. We find that the upper limit on the quartic coupling derived in [42] is orders of magnitude weaker than the one allowed by the Milky Way satellites in Eq. (34). As a result, the quartic can always be chosen between these bounds so as to not suffer from either constraints, and in the spirit of being conservative, we do not display the superradiance limits.

D. Neutrino free streaming

The Yukawa interaction in Eq. (5) enables $\phi\nu \to \phi\nu$ scattering, which can modify the neutrino free streaming length and affect CMB observables. Since active neutrinos do not couple directly to ϕ, the cross section for this process requires two Dirac mass insertions and scales as $\sigma \sim y_\phi^4 m_D^2/T^4$. Ensuring that the typical neutrino not scatter in a Hubble time at recombination $T_{rec} \sim 0.1$ eV requires

$$y_\phi \lesssim \left(\frac{1.66\sqrt{g_\star}T_{rec}^3 T_0^3 m_\phi}{\rho_{DM,0} m_{Pl} m_D^2}\right)^{1/4} \tag{35}$$

$$\approx 10^{-11}\left(\frac{10 \text{ meV}}{m_D}\right)^{1/2}\left(\frac{m_\phi}{1 \text{ eV}}\right)^{1/4}, \tag{36}$$

where $g_\star = 3.36$ is the number of effective relativistic species at recombination and $T_0 = 2.72$ K is the present day CMB temperature. This bound is shown in Fig. 1 as the green shaded region.

E. CMB/BBN

In this section, we investigate the effects of the scalar field in the early Universe, specifically, active to sterile oscillations, which increase the effective number of neutrino species ΔN_{eff}.

1. Cosmological field density

If the relic density was set by the misalignment mechanism, then the DM density grows as T^3 and remains as nonrelativistic DM until the temperature T_H when $m_\phi = 3H(T_H)$, where H is the Hubble parameter. Above this temperature, the field is constant due to Hubble friction and only contributes to the vacuum energy, so we have

$$\rho_\phi(T) = \rho_\phi(T_0)\left(\frac{g_{\star,S}(T_0)}{g_{\star,S}(T)}\right)\left(\frac{\min(T, T_H)}{T_0}\right)^3, \quad (37)$$

where $T_0 = 2.72$ K is the present day CMB temperature and $\rho_\phi(T_0) = \Omega_{\mathrm{dm}}\rho_c$ is the cosmological DM density, which is related to the local overdensity via $\rho_\phi(T_0) \approx 3 \times 10^{-6}\rho_\phi^\odot$. In what follows, we insert Eq. (37) into $m_M(T) = y_\phi\phi(T)/2$ using Eq. (2) to model the Majorana mass as function of cosmic temperature.

2. Cosmological sterile neutrino production

To compute the early Universe sterile neutrino yield, it is convenient to define r_β as the ratio of active/sterile momentum moments

$$r_\beta \equiv \frac{\langle p^\beta \rangle_s}{\langle p^\beta \rangle_a}, \quad (38)$$

where angular brackets $\langle \cdots \rangle_{s,a}$ denote a thermal average over the sterile and active distributions, respectively. Generalizing the formalism of Ref. [43], r_β satisfies the Boltzmann equation

$$\frac{dr_\beta}{dT} = -\frac{1}{2HT\langle p^\beta \rangle_a}\int \frac{d^3p}{(2\pi)^3}\frac{p^\beta\Gamma\sin^2(2\theta_M)}{e^{p/T}+1}, \quad (39)$$

where $\Gamma = \frac{7\pi}{24}G_F^2 p T^4$, and the mixing angle is

$$\sin^2(2\theta_M) = \frac{\sin^2(2\theta_0)}{[\cos(2\theta_0) - 2pV_{\mathrm{eff}}/\Delta m^2]^2 + \sin^2(2\theta_0)}, \quad (40)$$

where the effective matter potential for each flavor $a = e$, μ, τ can be written as

$$V_{\mathrm{eff}}^a = \pm C_1\eta G_F T^3 - \frac{C_2^a}{\alpha}G_F^2 T^4 p, \quad (41)$$

where $\eta = (n_L - n_{\bar{L}})/n_\gamma = 6 \times 10^{-10}$ is the lepton asymmetry, $C_1 = 0.95$, $C_2^e \approx 0.61$, $C_2^{\mu,\tau} \approx 0.17$, and the $\pm$ refer to neutrinos and antineutrinos [44]. Here the vacuum mixing angle θ_0 in Eq. (40) is ϕ dependent,

$$\theta_0 = \tan^{-1}\left(\frac{y_\phi\sqrt{2\rho_\phi}}{m_D m_\phi}\right), \quad (42)$$

where we have used Eqs. (6) and (9). Note that the first two moments of the active neutrino distribution yield the number and energy densities [$\langle p^0 \rangle_a = n_a$, $\langle p^1 \rangle_a = \rho_a$].

In the following subsections, we derive detailed ΔN_{eff} limits from BBN and CMB based on $\nu_a \to \nu_s$ oscillations around $T \approx$ MeV; later oscillations do not affect light element yields or the Hubble rate. The oscillation probability is maximized when the argument of Eq. (4) is order 1, implying

$$\frac{\delta m^2 L}{T} \sim \frac{m_D m_M}{G_F^2 T^6} \sim \left(\frac{y_\phi}{10^{-29}}\right)\left(\frac{m_D}{10\,\mathrm{meV}}\right)\left(\frac{10^{-12}\,\mathrm{eV}}{m_\phi}\right), \quad (43)$$

where we have used $\delta m^2 = m_D m_M$ and $m_M \sim y_\phi\phi$ from Eq. (6), $\phi \sim \sqrt{\rho_\phi}/m_\phi \propto T^{3/2}$ from Eq. (2), and approximated $L \sim (G_F^2 T^5)^{-1}$ as the neutrino mean free path, setting $T = $ MeV throughout. Thus, the blueshifted DM density at BBN greatly enhances the neutrino Majorana mass and yields on order 1 oscillation probability for extremely feeble couplings $y_\phi \sim \mathcal{O}(10^{-29})$. Note that, in our numerical study below, we use the full temperature dependence from Eq. (37), which also accounts for the Hubble damped regime when $T > T_H$ and is relevant for the smallest values of m_ϕ we consider.

However, from Eq. (37), for sufficiently large values of y_ϕ and ρ_ϕ, $m_M > m_D$, so neutrinos are no longer pseudo-Dirac fermions at high temperatures. In this regime, $\nu_a \to \nu_s$ oscillations are sharply suppressed as $\theta_0 \to \pi/2$ in Eq. (42), so there is a ceiling to the couplings that can be probed in the early Universe; this effect yields concave regions for the BBN/CMB regions in Fig. 1.

3. Extracting the CMB ΔN_{eff} limit

For temperatures before active neutrino decoupling, sterile neutrinos produced via $\nu_a \to \nu_s$ oscillations contribute to ΔN_{eff}, which can be constrained using cosmic microwave background anisotropy data. Oscillations that take place after neutrino decoupling interchange active and sterile states, but do not contribute to ΔN_{eff}. In terms of r in Eq. (39), sterile production via a flavor oscillations predicts

$$\Delta N_{\mathrm{eff}}^{\mathrm{CMB}} = r_1(T_{\mathrm{dec}}^{\nu_a}), \quad (44)$$

where $T_{\mathrm{dec}}^{\nu_e} \approx 3.2$ and $T_{\mathrm{dec}}^{\nu_\mu,\nu_\tau} \approx 5.34$ MeV are the temperatures of $\nu_a\bar{\nu}_a \to e^+e^-$ chemical decoupling [44]. Assuming the ΛCDM cosmological model, the Planck Collaboration constraints $\Delta N_{\mathrm{eff}} \lesssim 0.28$ [37] and we show this constraint in Fig. 1 as the blue shaded region alongside projections from future measurements with CMB-S4 [45].

4. BBN ΔN_{eff} limit

A nonzero ΔN_{eff} from sterile production also yields a larger initial neutron/proton fraction at the onset of BBN, which increases the primordial helium fraction. As in Eq. (44), for ϕ coupled to $\nu_{\mu,\tau}$, the effect on BBN arises purely from the expansion rate via

$$\Delta N_{\mathrm{eff}}^{\mathrm{BBN}} = r_1(T_{\mathrm{dec}}^{\nu_{\mu,\tau}}), \quad (45)$$

where r_1 is the solution to Eq. (39) with $\beta = 1$ evaluated at decoupling, assuming no initial population of steriles. The blue contour of Fig. 1 (right panel) shows parameter space

where $\Delta N_{\rm eff}^{\rm BBN} > 0.5$ [46,47] for ϕ coupled to the ν_3 mass eigenstate, implying oscillations from ν_μ and ν_τ flavor states.

However, for $\nu_e \to \nu_s$ oscillations, there are two distinct effects that impact the n/p ratio: oscillations before ν_e chemical decoupling at $T_{\rm dec}^{\nu_e} \approx 3.2$ MeV change the expansion rate as above, and oscillations after decoupling *deplete* the ν_e density. Both effects can be captured with a shift[3] in the effective Fermi constant via

$$G_F^2 \to \frac{1}{2} G_F^2 [2 + r_2(T_{\rm dec}^{\nu_e}) - r_2(T_{\rm nuc})] \qquad (46)$$

and a simultaneous shift in $g_\star$ via

$$g_\star \to g_{\star,\rm SM} + \frac{7}{4} r_1(T_{\rm dec}^{\nu_e}), \qquad (47)$$

where $g_{\star,\rm SM} = 10.75$ during BBN, and $T_{\rm nuc} \approx 0.8$ MeV is the temperature at which nucleon interconversion freezes out in the SM. We can economically capture both effects with an equivalent $\Delta N_{\rm eff}^{\rm BBN}$ [48] to obtain

$$\Delta N_{\rm eff}^{\rm BBN} \approx r_1(T_{\rm dec}^{\nu_e}) + \frac{4}{7} g_{\star,\rm SM} [r_2(T_{\rm nuc}) - r_2(T_{\rm dec}^{\nu_e})]. \qquad (48)$$

In Fig. 1 (left panel), the blue shaded region shows the BBN exclusion for which $\Delta N_{\rm eff}^{\rm BBN} > 0.5$.

VI. CONCLUSIONS

In this paper, we have presented the first cosmologically viable model in which neutrino masses acquire time

---

[3]Note that $\langle p^2 \rangle_a \propto T^5$, which sets the weak scattering rate $\Gamma \sim G_F^2 T^5$, so $r_2 = \langle p^2 \rangle_s / \langle p^2 \rangle_s$ yields the fractional departure from this rate.

dependence through their coupling to ultralight dark matter. In our scenario, the DM interaction sets the right-handed neutrino Majorana mass and neutrinos are pseudo-Dirac fermions with small mass splittings between active and sterile states. Since in the pseudo-Dirac regime the mixing angle between active and sterile is maximal, we extract limits on *ultrafeeble* Yukawa couplings between DM and right-handed neutrinos, constraining values of order $y_\phi \sim 10^{-30}$ for $m_\phi \sim 10^{-19}$ eV in the fuzzy DM regime [49]; for such small couplings, the ϕ mediated Yukawa force between right-handed neutrinos is comparable to that of gravity.

Throughout our analysis, we have emphasized bounds from solar and atmospheric neutrino oscillations, large scale structure, and the CMB/BBN eras. However, additional limits on this scenario may also be extracted by studying cosmic ray propagation [18] or diffuse supernova background neutrinos [50,51], which we leave for future work.

[1] J.-P. Uzan, The fundamental constants and their variation: Observational and theoretical status, Rev. Mod. Phys. **75**, 403 (2003).

[2] M. M. Reynoso and O. A. Sampayo, Propagation of high-energy neutrinos in a background of ultralight scalar dark matter, Astropart. Phys. **82**, 10 (2016).

[3] A. Berlin, Neutrino Oscillations as a Probe of Light Scalar Dark Matter, Phys. Rev. Lett. **117**, 231801 (2016).

[4] G. Krnjaic, P. A. N. Machado, and L. Necib, Distorted neutrino oscillations from time varying cosmic fields, Phys. Rev. D **97**, 075017 (2018).

[5] V. Brdar, J. Kopp, J. Liu, P. Prass, and X.-P. Wang, Fuzzy dark matter and nonstandard neutrino interactions, Phys. Rev. D **97**, 043001 (2018).

[6] H. Davoudiasl, G. Mohlabeng, and M. Sullivan, Galactic dark matter population as the source of neutrino masses, Phys. Rev. D **98**, 021301 (2018).

[7] J. Liao, D. Marfatia, and K. Whisnant, Light scalar dark matter at neutrino oscillation experiments, J. High Energy Phys. 04 (2018) 136.

[8] F. Capozzi, I. M. Shoemaker, and L. Vecchi, Neutrino oscillations in dark backgrounds, J. Cosmol. Astropart. Phys. 07 (2018) 004.

[9] G.-Y. Huang and N. Nath, Neutrinophilic axion-like dark matter, Eur. Phys. J. C **78**, 922 (2018).

[10] Y. Farzan, Ultra-light scalar saving the $3+1$ neutrino scheme from the cosmological bounds, Phys. Lett. B **797**, 134911 (2019).

[11] J. M. Cline, Viable secret neutrino interactions with ultralight dark matter, Phys. Lett. B **802,** 135182 (2020).

[12] A. Dev, P. A. N. Machado, and P. Martínez-Miravé, Signatures of ultralight dark matter in neutrino oscillation experiments, J. High Energy Phys. 01 (2007) 094.

[13] M. Losada, Y. Nir, G. Perez, and Y. Shpilman, Probing scalar dark matter oscillations with neutrino oscillations, J. High Energy Phys. 04 (2017) 030.

[14] G.-y. Huang and N. Nath, Neutrino meets ultralight dark matter: $0\nu\beta\beta$ decay and cosmology, J. Cosmol. Astropart. Phys. 05 (2022) 034.

[15] E. J. Chun, Neutrino transition in dark matter, arXiv:2112.05057.

[16] A. de Gouvea, TASI lectures on neutrino physics, in *Theoretical Advanced Study Institute in Elementary Particle Physics: Physics in D ≧ 4* (2004), pp. 197–258, arXiv:hep-ph/0411274.

[17] P. F. de Salas and A. Widmark, Dark matter local density determination: Recent observations and future prospects, Rep. Prog. Phys. **84,** 104901 (2021).

[18] A. de Gouvea, W.-C. Huang, and J. Jenkins, Pseudo-Dirac neutrinos in the new Standard Model, Phys. Rev. D **80,** 073007 (2009).

[19] M. Cirelli, G. Marandella, A. Strumia, and F. Vissani, Probing oscillations into sterile neutrinos with cosmology, astrophysics and experiments, Nucl. Phys. **B708,** 215 (2005).

[20] S. J. Parke, Nonadiabatic Level Crossing in Resonant Neutrino Oscillations, Phys. Rev. Lett. **57,** 1275 (1986).

[21] J. Hosaka *et al.* (Super-Kamiokande Collaboration), Solar neutrino measurements in Super-Kamiokande-I, Phys. Rev. D **73,** 112001 (2006).

[22] J. P. Cravens *et al.* (Super-Kamiokande Collaboration), Solar neutrino measurements in Super-Kamiokande-II, Phys. Rev. D **78,** 032002 (2008).

[23] B. Aharmim *et al.* (SNO Collaboration), Low energy threshold analysis of the phase I and phase II data sets of the Sudbury Neutrino Observatory, Phys. Rev. C **81,** 055504 (2010).

[24] K. Abe *et al.* (Super-Kamiokande Collaboration), Solar neutrino results in Super-Kamiokande-III, Phys. Rev. D **83,** 052010 (2011).

[25] G. Bellini *et al.*, Precision Measurement of the ^7Be Solar Neutrino Interaction Rate in Borexino, Phys. Rev. Lett. **107,** 141302 (2011).

[26] B. Aharmim *et al.* (SNO Collaboration), Combined analysis of all three phases of solar neutrino data from the Sudbury Neutrino Observatory, Phys. Rev. C **88,** 025501 (2013).

[27] A. Gando *et al.* (KamLAND Collaboration), Reactor on-off antineutrino measurement with KamLAND, Phys. Rev. D **88,** 033001 (2013).

[28] G. Bellini *et al.* (Borexino Collaboration), Final results of Borexino phase-I on low energy solar neutrino spectroscopy, Phys. Rev. D **89,** 112007 (2014).

[29] K. Abe *et al.* (Super-Kamiokande Collaboration), Solar neutrino measurements in Super-Kamiokande-IV, Phys. Rev. D **94,** 052010 (2016).

[30] P. Zyla *et al.* (Particle Data Group), Review of particle physics, Prog. Theor. Exp. Phys. **2020,** 083C01 (2020).

[31] N. Dalal and A. Kravtsov, Excluding fuzzy dark matter with sizes and stellar kinematics of ultrafaint dwarf galaxies, Phys. Rev. D **106,** 063517 (2022).

[32] D. Harlow, B. Heidenreich, M. Reece, and T. Rudelius, The weak gravity conjecture: A review, arXiv:2201.08380.

[33] Y. Fukuda *et al.* (Super-Kamiokande Collaboration), Evidence for Oscillation of Atmospheric Neutrinos, Phys. Rev. Lett. **81,** 1562 (1998).

[34] R. Wendell *et al.* (Super-Kamiokande Collaboration), Atmospheric neutrino oscillation analysis with subleading effects in Super-Kamiokande I, II, and III, Phys. Rev. D **81,** 092004 (2010).

[35] E. Richard *et al.* (Super-Kamiokande Collaboration), Measurements of the atmospheric neutrino flux by Super-Kamiokande: Energy spectra, geomagnetic effects, and solar modulation, Phys. Rev. D **94,** 052001 (2016).

[36] K. Abe *et al.* (Super-Kamiokande Collaboration), Atmospheric neutrino oscillation analysis with external constraints in Super-Kamiokande I-IV, Phys. Rev. D **97,** 072001 (2018).

[37] N. Aghanim *et al.* (Planck Collaboration), Planck 2018 results. VI. Cosmological parameters, Astron. Astrophys. **641,** A6 (2020); **652,** C4(E) (2021).

[38] T. Tenkanen, Dark Matter from Scalar Field Fluctuations, Phys. Rev. Lett. **123,** 061302 (2019).

[39] S. Das and E. O. Nadler, Constraints on the epoch of dark matter formation from Milky Way satellites, Phys. Rev. D **103,** 043517 (2021).

[40] M. S. Turner, Coherent scalar field oscillations in an expanding Universe, Phys. Rev. D **28,** 1243 (1983).

[41] A. Arvanitaki, S. Dimopoulos, S. Dubovsky, N. Kaloper, and J. March-Russell, String axiverse, Phys. Rev. D **81,** 123530 (2010).

[42] M. Baryakhtar, M. Galanis, R. Lasenby, and O. Simon, Black hole superradiance of self-interacting scalar fields, Phys. Rev. D **103,** 095019 (2021).

[43] S. Dodelson and L. M. Widrow, Sterile-Neutrinos as Dark Matter, Phys. Rev. Lett. **72,** 17 (1994).

[44] A. D. Dolgov and F. L. Villante, BBN bounds on active sterile neutrino mixing, Nucl. Phys. **B679,** 261 (2004).

[45] K. N. Abazajian *et al.* (CMB-S4 Collaboration), CMB-S4 science book, first edition, arXiv:1610.02743.

[46] N. Blinov, K. J. Kelly, G. Z. Krnjaic, and S. D. McDermott, Constraining the Self-Interacting Neutrino Interpretation of the Hubble Tension, Phys. Rev. Lett. **123,** 191102 (2019).

[47] S. Gariazzo, P. F. de Salas, O. Pisanti, and R. Consiglio, PArthENoPE revolutions, Comput. Phys. Commun. **271,** 108205 (2022).

[48] R. Barbieri and A. Dolgov, Bounds on sterile-neutrinos from nucleosynthesis, Phys. Lett. B **237,** 440 (1990).

[49] W. Hu, R. Barkana, and A. Gruzinov, Cold and Fuzzy Dark Matter, Phys. Rev. Lett. **85,** 1158 (2000).

[50] A. de Gouvêa, I. Martinez-Soler, Y. F. Perez-Gonzalez, and M. Sen, The diffuse supernova neutrino background as a probe of late-time neutrino mass generation, Phys. Rev. D **106,** 103026 (2022).

[51] J. F. Beacom, The diffuse supernova neutrino background, Annu. Rev. Nucl. Part. Sci. **60,** 439 (2010).